A DFT INVESTIGATION ON THE ELECTROCHEMICAL REDUCTION OF CO_2 TO CO OVER DUAL PRECIOUS METAL ATOMS DECORATED GRAPHENE

NGHIÊN CỨU QUÁ TRÌNH KHỬ ĐIỆN HOÁ CO_2 THÀNH CO TRÊN CHẤT XÚC TÁC LƯỠNG NGUYÊN TỬ KIM LOẠI QUÝ GẮN TRÊN GRAPHENE BẰNG PHƯƠNG PHÁP DFT

Ho Viet Thang[1]*, Thong Le Minh Pham[2], Mai Van Bay[3], Nguyen Thi Minh Xuan[1]

[1]*The University of Danang - University of Science and Technology*
[2]*Duy Tan University*
[3]*The University of Danang - University of Science and Education*

*Corresponding author: hvthang@dut.udn.vn

Abstract - The CO_2 electrochemical reduction to CO on dual precious metal atoms M_2 (M_2 = Pt_2, Pd_2, and Pt_1Pd_1) decorated graphene (M_2/G) is investigated by using density functional theory with van der Waals corrections. The electronic structure analyses show that the dual precious metal atoms anchored graphene are able to activate CO_2 thanks to the charge transfer from metal atoms to the antibonding π^* orbital of CO_2. The activations of CO_2 on the dual precious metal atoms result in the bendings of adsorbed CO_2 compared to free CO_2. The calculated free energy changes demonstrate that the desorption of CO from the catalyst surfaces is the most thermodynamically unfavorable step in the electrochemical reduction of CO_2.

Key words - CO_2 reduction; graphene; dual precious metal atom; DFT.

Tóm tắt - Sự khử CO_2 điện hóa thành CO trên các lưỡng nguyên tử kim loại quý M_2 (M_2 = Pt_2, Pd_2 và Pt_1Pd_1) gắn trên graphene (M_2/G) được khảo sát bằng phương pháp lý thuyết phiếm hàm mật độ. Phân tích cấu trúc điện tử cho thấy, các lưỡng nguyên tử kim loại gắn trên graphene có khả năng hoạt hóa CO_2 nhờ vào sự chuyển điện tử từ các nguyên tử kim loại sang orbital phản liên kết π^* của CO_2. Quá trình hoạt hoá trên bề mặt chất xúc tác làm cho phân tử CO_2 bị bẻ cong so với dạng cấu trúc thẳng của phân tử CO_2 tự do. Kết quả tính toán biến thiên năng lượng tự do cho thấy sự giải hấp của CO là quá trình không thuận lợi nhất về mặt năng lượng trong cơ chế khử điện hoá của CO_2 thành CO.

Từ khóa - Sự khử CO_2; graphene; hai nguyên tử kim loại quý; DFT.

1. Introduction

The increasing consumption of fossil fuels (coal, oil, and natural gas) in various sectors including transportation, industrial and human activities causes serious problems to the environment, and CO_2 is main agent giving rise to climate change and the greenhouse effect [1], [2]. Thus, the conversion of CO_2 into useful compounds or feedstock materials for fuels (methanol, polycarbonate, methane) is one of the urgent tasks to reduce CO_2 concentration in the atmosphere [3]. Various methods have been investigated to minimize global carbon dioxide including carbon sequestration, biochemical, photocatalytic, thermochemical conversion and electrochemical reduction approaches [4]. Among these strategies, CO_2 electrochemical reduction is a promising approach to converting CO_2 into different value-added compounds such as CO, H_2, HCOOH, CH_4 [5]. However, CO_2 is a linear structure (O=C=O), an extremely stable compound [6], and importantly, the reduction of CO_2 to CO is very slow and difficult to take place without the catalysts. Therefore, finding a new catalyst with a highly active center is needed for speeding up the reduction reaction of CO_2. Various catalysts have been exploited, in which precious metals deposited on different supporting materials, such as metal oxides, metal-organic frameworks, zeolite, and graphene have been experimentally and theoretically investigated and exhibited as efficient materials for CO_2 electrochemical reduction [4]. However, the main drawback of using these precious metals is the high cost and not using completely these active metal sites. In recent years, single-atom catalysts have attracted huge attention in catalysts due to their maximum atomic utilization and high selectivity. Among the supporting materials, graphene is the most applied because of its unique properties such as large surface area, and high electron mobility [7]. Furthermore, it has been demonstrated that the deposition of metals on graphene surface is facile. It has been also demonstrated that the decoration of transition metals on graphene significantly enhances the adsorption and activation of CO_2 [6], [8]. The precious single atom metals such as Pt, Pd decorated graphene have been successfully synthesized and applied as catalysts for the hydrogenation of acetylene to ethylene, CO oxidation, methanol oxidation, and CO_2 transformation [9] – [14]. Especially, the CO_2 conversion was found to be more efficiency on dual metal atom catalysts than on single-atom catalysts due to the synergistic effect of the two active sites [7]. However, the nature of CO_2 activation on dual precious metal atoms decorated graphene have not been fully understood at the atomic scale. It was demonstrated that the high stability of the single metal atoms or dual metal atoms on graphene is due to the strong interactions with the defect sites or with decorated functional groups [13], [15]. The adsorptions of single metal atoms on pristine graphene have also been theoretically studied for the oxidation of CO and NO [16], [17]. Thus, in this study we applied the dual metal atoms decorated graphene as

catalyst models for the CO_2 activation and electrochemical reduction of CO_2 to CO.

To be specific, we investigated CO_2 electrochemical reduction to CO on dual precious metal atoms including homoatomic dual atoms (Pt_2, Pd_2) and heteroatomic dual atoms (Pt_1Pd_1) anchored on graphene by means of the spin polarized density functional theory with van der Waals corrections. The electronic properties of graphene supported dual metal atoms and CO_2 electrochemical reduction pathways are characterized and analized to shed some light on the effect of different dual metal atoms on CO_2 reduction.

2. Method and models

All spin-polarized DFT calculations were performed by Vienna Ab initio Simulation Package (VASP) [18]. The exchange-correlation of electrons was described by the generalized gradient approximation within Perdew-Burke-Ernzerhof (PBE) functional [19]. The nuclei and core electrons interaction were described with projector augmented wave (PAW) [20], while the valence electrons explicitly included are $C(2s^2\ 2p^2)$, $Pd(4d^9\ 5s^1)$, $Pt(5d^9\ 6s^1)$, and $O\ (2s^2\ 2p^4)$. DFT-D3 method [21] was applied to describe the long-range interactions. The plane wave basis set with a cut off energy of 400 eV was used. A k-point mesh of $2\times2\times1$ was applied for the geometrical optimization and a denser k-points mesh of $4\times4\times1$ was used for the density of state (DOS) calculations [8]. The optimized structures were reached with the ionic force threshold of 0.01 eV/Å.

$7\times7\times1$ supercell of graphene containing 98 atoms [8] has been adopted to model the electronic properties of dual precious metal atoms anchored on graphene and the CO_2 electrochemical reduction. The binding energy (E_b in eV) of dual precious metal atoms on graphene (G) was determined by the following equation:

$$E_b = E(M_2/G) - E(G) - E(M_2)$$

where $E(M_2/G)$, $E(G)$, and $E(M_2)$ is the total energy of dual precious metal atoms M_2 (Pd_2, Pd_1Pt_1, Pt_2) on graphene, of bare graphene and of dual metal atoms in gas phase, respectively.

The CO_2 adsorption energy (E_{ads} in eV) on graphene or dual precious metal atoms anchored graphene was computed as:

$$E_{ads} = E(CO_2@S) - E(S) - E(CO_2)$$

where $E(CO_2@S)$, $E(S)$, and $E(CO_2)$ is the total energy of CO_2 bound to M_2/G or G; of M_2/G or G; of the isolated CO_2 molecule, respectively.

The charge density difference (ρ_{CDD}) [22] was calculated by the following equation:

$$\rho_{CDD} = \rho(CO_2@M_2/G) - \rho(M_2/G) - \rho(CO_2)$$

where $\rho(CO_2@M_2/G)$, $\rho(M_2/G)$, and $\rho(CO_2)$ is charge density of CO_2 bound to M_2/G, of M_2/G, and of CO_2 molecule obtained from adsorption complex geometry, respectively.

The effective charge of atoms was determined by using the Bader method [23], [24].

The change of free energy, ΔG was calculated by the following equation [25]:

$$\Delta G = \Delta E + \Delta G_{298K}$$

where, ΔE and ΔG_{298K} is the change of total energy and free energy correction at 298K, respectively. The free energy correction includes the zero-point energies and entropy [26].

Particularly, at the given step $\Delta E = E_{tot}(later-complexes) - E_{tot}(previous-complexes)$ and $\Delta G_{298K} = G_{298K}(later-complexes) - G_{298K}(previous-complexes) = \Delta ZPE + \Delta_{0-298K}H - T\Delta S$.

3. Results and Discussion

3.1. Electronic characteristics of dual precious metal atoms on graphene

Firstly, we considered all the possible sites of dual precious metal atoms on graphene including hollow, C-top, and C-C bridge sites. We found that the dual metal atoms prefer to reside at C-C bridge sites, and our results are in good agreement with the previous DFT study [27]. The electronic structure and structural parameters of these structures are presented in Table 1 and Figure 2. It can be seen from Table 1 that the binding energy of homoatomic dual atoms Pd_2 (-1.83 eV) is 0.76 eV stronger than its counterpart Pt_2 (-1.07 eV) on graphene. This indicates that the Pd_2 is more stable than Pt_2 when homoatomic dual atoms are deposited on graphene due to stronger metal-support interaction. The stronger binding of Pd_2 with graphene compared to Pt_2 is also evidenced by a shorter distance between metal and graphene (2.337 Å vs. 2.453 Å) and the amount of charge transfer to graphene. Particularly, the charge transfer from Pd to graphene is 0.14 |e| while that for the case of Pt is only 0.03 |e|. In addition, a better overlap of the valence band and conduction band of graphene with Pd_2 in DOS profile (Figure 2) further confirms the stronger binding of Pd_2 with graphene.
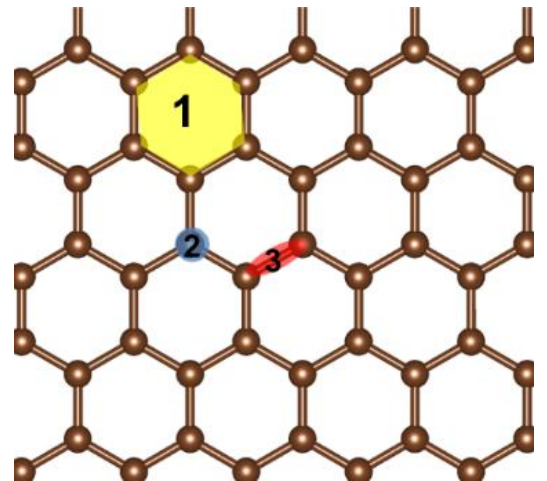

Figure 1. Top view of the optimized structure of graphene. The various adsorption sites on graphene are illustrated: (1) hollow, (2) C-top, and (3) C-C bridge

Regarding the heteroatomic dual atom anchored on graphene, the binding energy of Pd_1Pt_1 with graphene was calculated to be -1.40 eV which is smaller than for Pd_2

(-1.83 eV) but larger than for Pt_2 (-1.07 eV). For this structure, Pd and Pt are bound to graphene with a bond distance of 2.448 and 2.415 Å, respectively. The binding of Pd_1Pt_1 with graphene results in a charge transfer from Pd to graphene (Pd Bader charge of 0.18 |e|) and the mostly neutral charge on Pt (Pt Bader charge of -0.01 |e|).

Table 1. *Characteristics of dual precious metal atoms M_2 (M_2= Pd_2, Pt_2, Pd_1Pt_1) deposited on graphene. Binding energy, E_b, magnetic moment, Mag., Bader charge, Q(M), and the distance of precious atoms and graphene, d(Pd-G), d(Pt-G)*

System	E_b (eV)	Mag. (μ_B)	Q(Pd) (|e|)	Q(Pt) (|e|)	d(Pd-G) (Å)	d(Pt-G) (Å)
Pd_2/G	-1.83	0.00	0.14	-	2.377	-
Pt_2/G	-1.07	0.00	-	0.03	-	2.453
Pd_1Pt_1/G	-1.40	0.00	0.18	-0.01	2.448	2.415
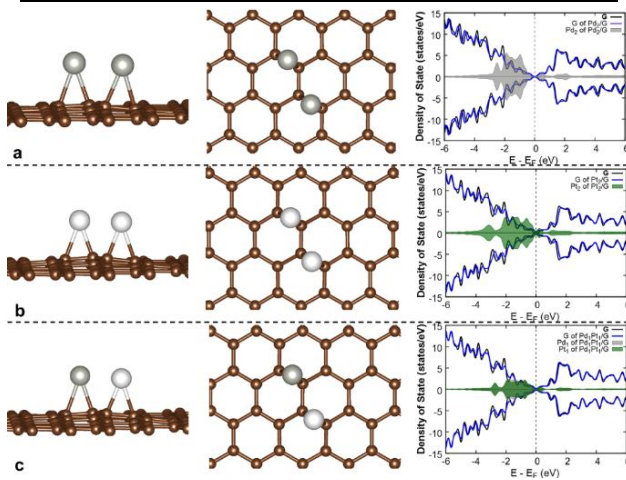
Figure 2. *Side view (left), top view (middle) and DOS (right) of a) Pd_2/G, b) Pt_2/G and c) Pd_1Pt_1/G. C, Pd, and Pt are brown, grey, white, and red spheres, respectively*

### 3.2. CO_2 adsorption on dual precious metal atoms anchored on graphene

CO_2 activation is the key step in the electrochemical reduction of CO_2 to CO. Therefore, we firstly consider the CO_2 activation on graphene-supported dual metal atoms. For a comparison, the adsorption of CO_2 on pristine graphene was also calculated. The DFT results indicate that CO_2 is physisorbed on pristine graphene with an adsorption energy of -0.14 eV (Table 2 and Figure 3a). The stability of CO_2 on pristine graphene is mainly dictated by van der Waals interactions. The weak adsorption of CO_2 on pristine graphene is also demonstrated by the geometrical structure of adsorbed CO_2 which remains unchanged compared to the gas-phase CO_2. The weak binding of CO_2 with pristine graphene is also indicated by the degenerate of π bonding and π^* antibonding molecule orbitals as illustrated in the DOS profile (Figure 3a).

The adsorption of CO_2 on dual metal atoms deposited on graphene is much stronger than on pristine graphene. It is noted that the adsorption energy of CO_2 on homoatomic dual atom Pt_2/G (-1.58 eV) is stronger than on Pd_2/G (-1.11 eV), while the value (-1.44 eV) for heteroatomic dual atoms Pd_1Pt_1/G is in the middle among the three. The relative binding strength of CO_2 with the surfaces is good agreement with the amount of charge transfer from the

graphene supported metal atoms to CO_2, and the higher charge transfer, the stronger adsorption energy. In particular, the amount of charge transfer from Pd_2/G, Pt_2/G, and Pd_1Pt_1/G to CO_2 is -0.41 |e|, -0.49 |e| and -0.44 |e|, respectively. This results in the elongation of the C=O bond length of about 0.1 Å and the bending of O-C-O angle from 180° (free CO_2) to 141° (on Pd_2/G), 131° (on Pt_2/G) and 135° (on Pd_1Pt_1/G) (Table 2). In addition, the charge transfer from dual metal atoms to CO_2 was also illustrated by the amount of charge accumulation on adsorbed CO_2 and by the large overlap of the DOS of metal atoms and CO_2 (Figure 3).

Table 2. *Characteristics of CO_2 adsorption on pristine and dual precious atoms M_2 anchored on Graphene. Adsorption energy, E_{ads}, magnetic moment, Mag., Bader charge of Pd, Q(Pd), of Pt, Q(Pt) of adsorbed dual atoms, Bader charge of adsorbed CO_2, Q(CO_2), bond angle of CO_2, ∠(OCO) and C-O bond lengths of CO_2, r(CO;CO)*

| System	E_{ads} (eV)	Mag. (μ_B)	Q(Pd) (|e|)	Q(Pt) (|e|)	Q(CO_2) (|e|)	∠(OCO) (°)	r(CO;CO) (Å)
G	-0.14	-	-		0.00	180	1.177;1.177
Pd_2/G	-1.11	0.00	0.28		-0.41	141	1.231;1.257
Pt_2/G	-1.58	0.00	-	0.24	-0.49	131	1.225;1.320
Pd_1Pt_1/G	-1.44	0.00	0.26	0.24	-0.44	135	1.222;1.290
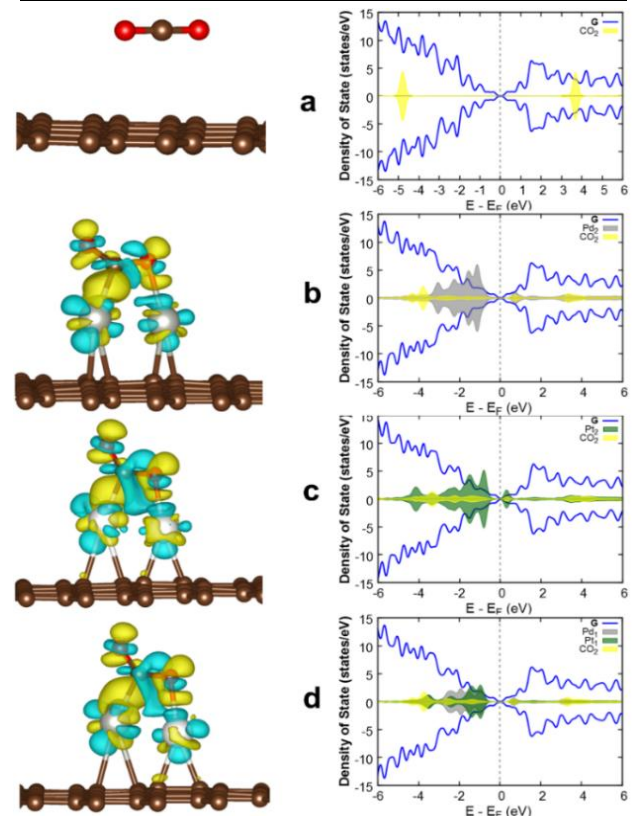
Figure 3. *Side view (left) with charge density difference and DOS (right) of CO_2 adsorbed on a) G, b) Pd_2/G, c) Pt_2/G, and d) Pd_1Pt_1/G. Transparent yellow and blue with an isosurface level of 0.003 |e|.bohr^{-3} are charge accumulation and charge depletion, respectively. C, Pd, Pt, and O are brown, grey, white, and red spheres, respectively*

To sum up, the amount of charge transfer from metal atoms to CO_2 is an important factor that governs the activation of CO_2 and this is the main criteria we should consider when designing new materials for CO_2 activation.

3.3. Free energy diagram for the pathway of the electrochemical reduction of CO_2 to CO

To gain insights into the catalytic activity of graphene supported dual metal atoms toward CO_2 conversion, the free energy profile of the electrochemical reduction of CO_2 to CO was also calculated [25]. It is widely known that the CO_2 electrochemical reduction is a competing reaction with the hydrogen evolution reaction (HER). However, HER can be suppressed by increasing CO_2 pressure or enhancing the adsorption of CO_2 on the catalyst surfaces, or using alloy catalysts [28], [29]. Therefore, for the sake of simplicity, we assumed that the CO_2 reduction is preferentially occurred on these catalysts. As shown in Figure 4, the reaction pathways take place through four elementary steps. The first one is the adsorption of CO_2 (CO_2 + supported dual metal atom (denoted as *) → *COO) in which CO_2 is bound to the dual metal atom via C and O. The second step is a proton-coupled electron transfer of activated COO forming *COOH (*COO + H^+ + e^- → *COOH). The third step is a proton-coupled electron transfer of *COOH releasing H_2O molecule and *CO (*COOH + H^+ + e^- → *CO +H_2O). The preference of two proton-coupled electron transfers to hydrogen atom transfer were considered as they have been demonstrated in the previous study [30]. The fourth step is the desorption of CO from the catalyst surface (*CO → CO + *). Figure 4 shows that the reaction energy of the first proton-coupled electron transfer is 0.07, 0.54, and 0.62 eV for Pt_2/G, Pd_1Pt_1/G, and Pd_2/G respectively which is consistent with the capability to activate CO_2 of these catalysts. It is also worth noting that the first proton-coupled electron transfer is endergonic while the second proton-coupled electron transfer is exergonic on M_2/G. Among the four steps, the desorption of CO is the most unfavorable reaction with a large reaction energy of 1.46, 2.04 and 2.59 eV for Pt_1Pd_1/G, Pd_2/G and Pt_2/G respectively.
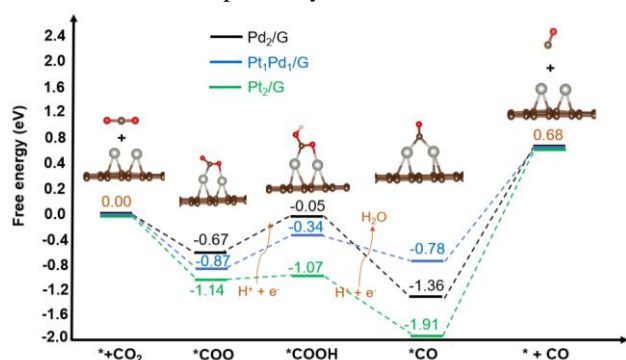
Figure 4. Free energy profile of electrochemical CO_2 reduction on Pd_2/G, Pt_1Pd_1/G, and Pt_2/G

4. Conclusions

The electronic and structural properties of dual precious metal atoms including homoatomic dual atoms (Pd_2 and Pt_2) and heteroatomic dual atoms (Pd_1Pt_1) anchored on graphene have been studied by DFT calculations with van der Waals corrections. The activation of CO_2 and the free energy of the pathway for CO_2 electrochemical reduction

on these graphene-supported dual metal atos were also investigated. The DFT results show that the binding strength of dual metal atoms with graphene follows the order: Pt_2/G < Pd_1Pt_1/G < Pd_2/G. Moreover, the adsorption energy of CO_2 on the surfaces was found to be in reverse order: Pd_2/G < Pd_1Pt_1/G < Pt_2/G. The theoretical results also demonstrate that desorption of CO from the catalyst surface is the most thermodynamically unfavorable step in the electrochemical reduction of CO_2. This study provides a background for designing nano catalysts for the electrochemical reduction of CO_2.

REFERENCES

[1] T. R. Anderson, E. Hawkins, and P. D. Jones, "CO2, the greenhouse effect and global warming: from the pioneering work of Arrhenius and Callendar to today's Earth System Models", *Endeavour*, vol. 40, no. 3, pp. 178–187, Sep. 2016, doi: 10.1016/j.endeavour.2016.07.002.

[2] "The greenhouse effect", *British Geological Survey*. https://www.bgs.ac.uk/discovering-geology/climate-change/how-does-the-greenhouse-effect-work/ (accessed Aug. 11, 2022).

[3] B. Yao *et al.*, "Transforming carbon dioxide into jet fuel using an organic combustion-synthesized Fe-Mn-K catalyst", *Nat Commun*, vol. 11, no. 1, Art. no. 1, Dec. 2020, doi: 10.1038/s41467-020-20214-z.

[4] A. Saravanan *et al.*, "A comprehensive review on different approaches for CO2 utilization and conversion pathways", *Chemical Engineering Science*, vol. 236, p. 116515, Jun. 2021, doi: 10.1016/j.ces.2021.116515.

[5] G. Centi and S. Perathoner, "Opportunities and prospects in the chemical recycling of carbon dioxide to fuels", *Catalysis Today*, vol. 148, no. 3, pp. 191–205, Nov. 2009, doi: 10.1016/j.cattod.2009.07.075.

[6] Z. Luo, Y. Su, R. Li, X. Chen, and T. Wang, "Effect of Inert Gas CO2 on Deflagration Pressure of CH4/CO", *ACS Omega*, vol. 5, no. 36, pp. 23002–23008, Sep. 2020, doi: 10.1021/acsomega.0c02686.

[7] Y. Li, H. Su, S. H. Chan, and Q. Sun, "CO2 Electroreduction Performance of Transition Metal Dimers Supported on Graphene: A Theoretical Study", *ACS Catal.*, vol. 5, no. 11, pp. 6658–6664, Nov. 2015, doi: 10.1021/acscatal.5b01165.

[8] A. Sihag *et al.*, "DFT Insights into Comparative Hydrogen Adsorption and Hydrogen Spillover Mechanisms of Pt4/Graphene and Pt4/Anatase (101) Surfaces", *J. Phys. Chem. C*, vol. 123, no. 42, pp. 25618–25627, Oct. 2019, doi: 10.1021/acs.jpcc.9b04419.

[9] S. A. Wella, Y. Hamamoto, Suprijadi, Y. Morikawa, and I. Hamada, "Platinum single-atom adsorption on graphene: a density functional theory study", *Nanoscale Adv.*, vol. 1, no. 3, pp. 1165–1174, Mar. 2019, doi: 10.1039/C8NA00236C.

[10] R. Krishnan, S.-Y. Wu, and H.-T. Chen, "Single Pt atom supported on penta-graphene as an efficient catalyst for CO oxidation", *Phys. Chem. Chem. Phys.*, vol. 21, no. 23, pp. 12201–12208, Jun. 2019, doi: 10.1039/C9CP02306B.

[11] S. Sun *et al.*, "Single-atom Catalysis Using Pt/Graphene Achieved through Atomic Layer Deposition", *Sci Rep*, vol. 3, no. 1, Art. no. 1, May 2013, doi: 10.1038/srep01775.

[12] Q. Liu *et al.*, "In situ immobilization of isolated Pd single-atoms on graphene by employing amino-functionalized rigid molecules and their prominent catalytic performance", *Catal. Sci. Technol.*, vol. 10, no. 2, pp. 450–457, Jan. 2020, doi: 10.1039/C9CY02110H.

[13] Q. Luo, W. Zhang, C.-F. Fu, and J. Yang, "Single Pd atom and Pd dimer embedded graphene catalyzed formic acid dehydrogenation: A first-principles study", *International Journal of Hydrogen Energy*, vol. 43, no. 14, pp. 6997–7006, Apr. 2018, doi: 10.1016/j.ijhydene.2018.02.129.

[14] S. Zhou *et al.*, "Pd Single-Atom Catalysts on Nitrogen-Doped

Graphene for the Highly Selective Photothermal Hydrogenation of Acetylene to Ethylene", *Advanced Materials*, vol. 31, no. 18, p. 1900509, 2019, doi: 10.1002/adma.201900509.

[15] H. He, C. Morrissey, L. A. Curtiss, and P. Zapol, "Graphene-Supported Monometallic and Bimetallic Dimers for Electrochemical CO2 Reduction", *J. Phys. Chem. C*, vol. 122, no. 50, pp. 28629–28636, Dec. 2018, doi: 10.1021/acs.jpcc.8b07887.

[16] P. Yan, S. Shu, X. Shi, and J. Li, "Promotion effect of Au single-atom support graphene for CO oxidation", *Chinese Chemical Letters*, vol. 33, no. 11, pp. 4822–4827, Nov. 2022, doi: 10.1016/j.cclet.2022.01.032.

[17] Y. Tang *et al.*, "Comparative Study of NO and CO Oxidation Reactions on Single-Atom Catalysts Anchored Graphene-like Monolayer", *ChemPhysChem*, vol. 22, no. 6, pp. 606–618, 2021, doi: 10.1002/cphc.202001021.

[18] G. Kresse and J. Furthmüller, "Efficiency of ab-initio total energy calculations for metals and semiconductors using a plane-wave basis set", *Computational Materials Science*, Jul. 1996, doi: 10.1016/0927-0256(96)00008-0.

[19] J. P. Perdew, K. Burke, and M. Ernzerhof, "Generalized Gradient Approximation Made Simple", *Phys. Rev. Lett.*, vol. 77, no. 18, pp. 3865–3868, Oct. 1996, doi: 10.1103/PhysRevLett.77.3865.

[20] G. Kresse and D. Joubert, "From ultrasoft pseudopotentials to the projector augmented-wave method", *Phys. Rev. B*, vol. 59, no. 3, pp. 1758–1775, Jan. 1999, doi: 10.1103/PhysRevB.59.1758.

[21] S. Grimme, J. Antony, S. Ehrlich, and H. Krieg, "A consistent and accurate ab initio parametrization of density functional dispersion correction (DFT-D) for the 94 elements H-Pu", *J. Chem. Phys.*, vol. 132, no. 15, p. 154104, Apr. 2010, doi: 10.1063/1.3382344.

[22] D. Tozini, M. Forti, P. Gargano, P. R. Alonso, and G. H. Rubiolo, "Charge Difference Calculation in Fe/Fe3O4 Interfaces from DFT Results", *Procedia Materials Science*, vol. 9, pp. 612–618, Jan. 2015, doi: 10.1016/j.mspro.2015.05.037.

[23] G. Henkelman, A. Arnaldsson, and H. Jónsson, "A fast and robust algorithm for Bader decomposition of charge density", *Computational Materials Science*, vol. 36, no. 3, pp. 354–360, Jun. 2006, doi: 10.1016/j.commatsci.2005.04.010.

[24] W. Tang, E. Sanville, and G. Henkelman, "A grid-based Bader analysis algorithm without lattice bias", *J. Phys.: Condens. Matter*, vol. 21, no. 8, p. 084204, Jan. 2009, doi: 10.1088/0953-8984/21/8/084204.

[25] Y. Li, C. Chen, R. Cao, Z. Pan, H. He, and K. Zhou, "Dual-atom Ag2/graphene catalyst for efficient electroreduction of CO2 to CO", *Applied Catalysis B: Environmental*, vol. 268, p. 118747, Jul. 2020, doi: 10.1016/j.apcatb.2020.118747.

[26] A. A. Peterson, F. Abild-Pedersen, F. Studt, J. Rossmeisl, and J. K. Nørskov, "How copper catalyzes the electroreduction of carbon dioxide into hydrocarbon fuels", *Energy Environ. Sci.*, vol. 3, no. 9, pp. 1311–1315, Aug. 2010, doi: 10.1039/C0EE00071J.

[27] C. R. C. Rêgo, P. Tereshchuk, L. N. Oliveira, and J. L. F. Da Silva, "Graphene-supported small transition-metal clusters: A density functional theory investigation within van der Waals corrections", *Phys. Rev. B*, vol. 95, no. 23, p. 235422, Jun. 2017, doi: 10.1103/PhysRevB.95.235422.

[28] H. Ooka, M. C. Figueiredo, and M. T. M. Koper, "Competition between Hydrogen Evolution and Carbon Dioxide Reduction on Copper Electrodes in Mildly Acidic Media", *Langmuir*, vol. 33, no. 37, pp. 9307–9313, Sep. 2017, doi: 10.1021/acs.langmuir.7b00696.

[29] M. Valenti *et al.*, "Suppressing H2 Evolution and Promoting Selective CO2 Electroreduction to CO at Low Overpotentials by Alloying Au with Pd", *ACS Catal.*, vol. 9, no. 4, pp. 3527–3536, Apr. 2019, doi: 10.1021/acscatal.8b04604.

[30] J. Song, E. L. Klein, F. Neese, and S. Ye, "The Mechanism of Homogeneous CO₂ Reduction by Ni(cyclam): Product Selectivity, Concerted Proton–Electron Transfer and C–O Bond Cleavage", *Inorg. Chem.*, vol. 53, no. 14, pp. 7500–7507, Jul. 2014, doi: 10.1021/ic500829p.